

Quantum Dense Coding with Atomic Qubits

T. Schaetz, M. D. Barrett,* D. Leibfried, J. Chiaverini, J. Britton, W. M. Itano, J. D. Jost, C. Langer, and D. J. Wineland

Time and Frequency Division, NIST, Boulder, Colorado 80305-3328, USA

(Received 27 April 2004; published 22 July 2004)

We report the implementation of quantum dense coding on individual atomic qubits with the use of two trapped ${}^9\text{Be}^+$ ions. The protocol is implemented with a complete Bell measurement that distinguishes the four operations used to encode two bits of classical information. We measure an average transmission fidelity of 0.85(1) and determine a channel capacity of 1.16(1).

DOI: 10.1103/PhysRevLett.93.040505

PACS numbers: 03.67.Lx, 32.80.Qk

Quantum dense coding [1] enables the communication of two bits of classical information with the transmission of one quantum bit or “qubit” (two-level quantum system). Two parties, Alice and Bob, each hold one qubit of a maximally entangled pair that has been previously prepared and distributed. With this starting point, Bob applies one of four possible unitary operations (each identified with the states of two classical bits) to his qubit and sends it to Alice. Alice then performs a Bell measurement [2] of both qubits; the outcomes of these measurements tell her which of the four operations Bob applied and the corresponding two-bit classical number.

Some of the elements of this protocol were first demonstrated in optics, where the qubit states were represented by a photon’s states of polarization [3]. The protocol was also simulated in nuclear magnetic resonance using temporal averaging [4]. Dense coding has been investigated theoretically [5–7] and experimentally [8,9] in the context of continuous variables. It has also been considered for more than two entangled bits [10–14] or entangled degrees of freedom [15], but here we limit our discussion to the case of two qubits.

In addition to the communication applications, implementation of the protocol serves as a benchmark for comparison of quantum information processing (QIP) in different physical realizations [16]. For trapped-ion QIP, it tests the viability of specific tools required for large-scale processing [17,18], including the ability to separate ion qubits and individually detect them. From a significantly different perspective, it can also be viewed as a demonstration of increased efficiency for determination of quantum dynamics using QIP. For example, Ref. [19] shows that the optimal way to estimate the effect of a black box (here a rotation operator) on one qubit, given only one use of the box, is to apply it to one qubit of a maximally entangled pair and measure both qubits in a Bell-state basis (see also Ref. [20]). This strategy coincides with the dense-coding protocol on two qubits.

We implement the basic protocol [1] using two trapped atomic ion qubits. We realize it on demand, without the need for postselection of data, and with the ability to transfer and detect all four states corresponding to Bob’s

two bits of classical information. Since the experiment was implemented in one location, it is not useful for long-distance communication, although it could be extended to this purpose with the use of efficient atom-photon coupling [21,22]. In our implementation (outlined in Fig. 1), after the pair of entangled qubits is prepared, we let Bob use the experimental apparatus first to encode his qubit; he then turns over the apparatus to Alice so she can decode the message using Bob’s and her qubit.

The qubits are composed of the $|F = 2, M_F = -2\rangle$ and $|F = 1, M_F = -1\rangle$ ground-state hyperfine levels of ${}^9\text{Be}^+$, labeled $|\downarrow\rangle$ and $|\uparrow\rangle$, respectively, where we use the formal equivalence between a two-level system and a spin- $\frac{1}{2}$ magnetic moment in a magnetic field (Bloch-vector representation) [23,24]. The ions are confined in a multizone linear rf-Paul trap similar to the one described in [25]. The ions are located on the axis of the trap structure, which we call the z direction. In a given trap zone, the

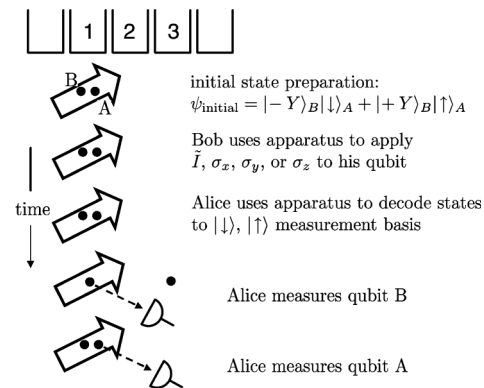


FIG. 1. Schematic diagram of the dense-coding implementation using atomic qubits. In the top part of the figure, the trap zones used in the experiment (not to scale) are designated with numbers. The z axis of the trap is parallel to the horizontal direction in the figure. The large arrows indicate schematically the laser beams used to implement the various operations. The dashed arrows indicate laser-induced fluorescence that is detected to determine the state of each ion ($|\downarrow\rangle$ fluoresces, $|\uparrow\rangle$ does not). To facilitate separate detection of qubits A and B, qubit B is measured first, then transferred to a nonfluorescing state, followed by detection of qubit A.

ions' motion along z can be described by normal modes corresponding to the center-of-mass (frequency $\omega_{\text{c.m.}}$) and "stretch" ($\omega_{\text{STR}} = \sqrt{3}\omega_{\text{c.m.}}$) modes, where the mode amplitudes are equal and in the same or opposite directions, respectively [26]. We adjust the trap potential to make $\omega_{\text{c.m.}}/2\pi = 3.71$ MHz, corresponding to a separation of $3.76 \mu\text{m}$ between ions. At the start of each experiment, the ions are laser cooled to the motional ground state and optically pumped into the internal states $|\downarrow\rangle_1 \otimes |\downarrow\rangle_2$ [26].

To implement the dense-coding protocol, we will need to realize single qubit gates (rotations) and a two-qubit universal logic gate [2]. For a single-qubit gate on ion i , the states $|\downarrow\rangle_i$ and $|\uparrow\rangle_i$ are coupled with stimulated Raman transitions excited with two laser beams (designated "blue" and "red" to indicate their relative detuning) that overlap both ions [27]. The k vectors of these beams are oriented such that \vec{k}_{blue} is approximately perpendicular to \vec{k}_{red} and $\Delta\vec{k} \equiv \vec{k}_{\text{blue}} - \vec{k}_{\text{red}} \simeq \sqrt{2}|\vec{k}_{\text{blue}}|\hat{z} \equiv \hat{z}2\pi/\lambda_{\text{eff}}$, where λ_{eff} is the effective wavelength of the Raman transition. By tuning the difference frequency of the laser beams to $(\omega_{\text{blue}} - \omega_{\text{red}})/2\pi = \omega_0/2\pi = (E_{\uparrow} - E_{\downarrow})/h \simeq 1.25$ GHz, we implement the rotation of the qubit state on the Bloch sphere

$$R_i(\theta, \phi_i) \equiv \begin{pmatrix} \cos\frac{\theta}{2} & -ie^{-i\phi_i}\sin\frac{\theta}{2} \\ -ie^{+i\phi_i}\sin\frac{\theta}{2} & \cos\frac{\theta}{2} \end{pmatrix}, \quad (1)$$

where we use the conventions

$$|\downarrow\rangle \equiv \begin{pmatrix} 0 \\ 1 \end{pmatrix}, \quad |\uparrow\rangle \equiv \begin{pmatrix} 1 \\ 0 \end{pmatrix}. \quad (2)$$

The angle θ is proportional to the duration of the Raman pulse. The phase factor $\phi_i = \Delta\vec{k} \cdot \vec{x}_i + \phi_{\text{blue},i} - \phi_{\text{red},i}$ is the phase difference between the Raman beams at the position \vec{x}_i of the i th ion.

To implement a universal logic gate between the ions, the Raman laser beams can be configured to apply state-dependent optical dipole forces. We choose the polarizations of the beams so that these forces along the z direction are related by $\vec{F}_{\downarrow} = -2\vec{F}_{\uparrow}$ [28,29]. We adjust the frequency difference between the Raman beams and therefore the frequency of the optical dipole force to be equal to $\omega_{\text{STR}} + \delta$ ($|\delta| \ll \omega_{\text{STR}}$). With the above choice of $\omega_{\text{c.m.}}$, the ions are separated by a distance $17.0 \times \lambda_{\text{eff}}$, so that if the ions are in the opposite state, the dipole force can (off resonantly) excite the ions' stretch mode. (If they are in the same state, the stretch mode is not excited.) By applying these forces for a gate time $\tau_G = 2\pi/\delta$ and adjusting their magnitude appropriately, we realize a geometric phase gate G_ϕ , which implements the operation [29]

$$G_\phi : a|\downarrow\rangle|\downarrow\rangle + b|\downarrow\rangle|\uparrow\rangle + c|\uparrow\rangle|\downarrow\rangle + d|\uparrow\rangle|\uparrow\rangle \\ \rightarrow a|\downarrow\rangle|\downarrow\rangle + ib|\downarrow\rangle|\uparrow\rangle + ic|\uparrow\rangle|\downarrow\rangle + d|\uparrow\rangle|\uparrow\rangle. \quad (3)$$

We will need to implement single-qubit rotations on one ion without changing the state of the other ion; this can be accomplished in one trap zone even though the Raman beams overlap both ions. To see how this is done, consider the following example [18,30]. Suppose we want to prepare the state $(|\downarrow\rangle_1 + |\uparrow\rangle_1) \otimes |\downarrow\rangle_2$ from the state $|\downarrow\rangle_1|\downarrow\rangle_2$ (for simplicity we omit normalization factors). We first apply a Raman pulse acting equally on both ions to implement the rotations $R_1(\frac{\pi}{4}, -\frac{\pi}{2}) \otimes R_2(\frac{\pi}{4}, -\frac{\pi}{2})$. The spins rotate into a state represented pictorially by $|\searrow\rangle_1|\searrow\rangle_2$. The spacing of the ions is now changed by $\lambda_{\text{eff}}/2$. A second Raman pulse of the same duration is applied to both qubits such that the laser phase on qubit 1 is the same, but because of the change in ion separation, the phase on qubit 2 is shifted by π . This carries out the operation $R_1(\frac{\pi}{4}, -\frac{\pi}{2}) \otimes R_2(\frac{\pi}{4}, +\frac{\pi}{2})$. Whence, qubit 2 is rotated back into its initial state while qubit 1 completes a $\theta = \frac{\pi}{2}$ rotation. Pictorially, application of the second Raman pulse implements the transformation $|\searrow\rangle_1|\searrow\rangle_2 \rightarrow |\rightarrow\rangle_1|\downarrow\rangle_2 = (|\downarrow\rangle_1 + |\uparrow\rangle_1) \otimes |\downarrow\rangle_2$. Generalizing this, we can apply the Pauli operators σ_x , σ_y , and σ_z to ion 1, which, up to global phase factors, correspond to the operators $R_1(\pi, 0)$, $R_1(\pi, \frac{\pi}{2})$, and $R_1(\pi, 0)R_1(\pi, \frac{\pi}{2})$ respectively.

Finally, we will need to detect both qubits individually in the $|\downarrow\rangle$, $|\uparrow\rangle$ basis. This is accomplished through state-dependent laser scattering ($|\downarrow\rangle$ fluoresces strongly, while $|\uparrow\rangle$ has negligible fluorescence [30]). We first separate qubits 1 and 2 into different trap zones as described in Ref. [25]. Qubit 1 remains in trap zone No. 1 (Fig. 1), while qubit 2 is transferred to an auxiliary zone (zone No. 3 in Fig. 1) located approximately $340 \mu\text{m}$ away. After detection of the state of qubit 1 [31], it is optically pumped to the state $|\downarrow\rangle_1$, and then a π pulse [$R_1(\pi, 0)$] is applied to transfer it to the state $|\uparrow\rangle_1$. Following this, both qubits are recombined in zone 1 and detected. Since qubit 1 does not fluoresce, we detect the state of ion 2 with less than 1% error due to the presence of ion 1.

With these tools, the dense-coding protocol is implemented as follows (Fig. 1). We first need to prepare the entangled state ψ_{initial} that Bob and Alice initially share. We let qubits 1 and 2 correspond to Bob's and Alice's qubits, respectively. We apply the operator $R_B(\frac{\pi}{2}, -\frac{\pi}{2}) \otimes R_A(\frac{\pi}{2}, -\frac{\pi}{2})$ followed by application of G_ϕ to the state $|\downarrow\rangle_B|\downarrow\rangle_A$. This leads to the transformations

$$|\downarrow\rangle_B|\downarrow\rangle_A \rightarrow (|\downarrow\rangle_B + |\uparrow\rangle_B)(|\downarrow\rangle_A + |\uparrow\rangle_A) \rightarrow \\ |-\rangle_B|\downarrow\rangle_A + |+\rangle_B|\uparrow\rangle_A \equiv \psi_{\text{initial}}, \quad (4)$$

where $|\pm\rangle$ correspond to Bloch eigenvectors aligned along the $\pm y$ directions with the properties $\sigma_y|\pm\rangle = \pm|\pm\rangle$. Therefore, the entangled state shared by Alice and Bob is a maximally entangled state, but for experimental convenience, they choose different bases for their initial states.

Bob, using the method of individual ion addressing described above, encodes his qubit with two classical bits of information by applying one of four operators according to the identification scheme: $(00) \leftrightarrow \tilde{I}_B$, $(01) \leftrightarrow \sigma_{yB}$, $(10) \leftrightarrow \sigma_{zB}$, and $(11) \leftrightarrow \sigma_{xB}$, where \tilde{I} is the identity operator. Now, Bob turns over his bit and the rest of the apparatus to Alice.

To decode the message that Bob encoded on his qubit, Alice takes both qubits and applies the operator G_ϕ followed by the operator $R_B(\frac{\pi}{2}, -\frac{\pi}{2}) \otimes R_A(\frac{\pi}{2}, -\frac{\pi}{2})$. Finally, Alice measures the states of each qubit as described above. Ideally, she finds the correlations between the detected states and Bob's two bit classical message according to $|\downarrow\rangle_B|\downarrow\rangle_A \leftrightarrow (00)$, $|\downarrow\rangle_B|\uparrow\rangle_A \leftrightarrow (01)$, $|\uparrow\rangle_B|\downarrow\rangle_A \leftrightarrow (10)$, and $|\uparrow\rangle_B|\uparrow\rangle_A \leftrightarrow (11)$.

The approximate durations of the various pulses in the experiment were as follows: $\pi/2 [R(\frac{\pi}{2}, \phi)]$ pulses, $0.7 \mu\text{s}$; π pulses, $1.4 \mu\text{s}$; G_ϕ , $10 \mu\text{s}$; and delays between pulses were a minimum of $2 \mu\text{s}$ (to avoid pulse overlaps from switching transients). The duration to change the separation of the ions by $\lambda_{\text{eff}}/2$ was $11 \mu\text{s}$, the duration to separate or recombine ions for individual detection was $250 \mu\text{s}$, the duration for fluorescence detection of each ion was $400 \mu\text{s}$, and the time to recool and optically pump the ions before each experiment was about 1 ms.

In practice, each of the above operations is imperfect. These imperfections are caused primarily by intensity fluctuations of both Raman beams, drifts in the detuning δ over the duration of many experiments, imperfect initial state preparation, and imperfect detection. A serious problem is caused by fluctuations of the ambient magnetic field. The qubit spin flip frequency $\omega_0/2\pi$ has magnetic field dependence of 2.1 MHz/G ; therefore, field fluctuations (up to 10 mG) can cause dephasing of the qubit states when averaged over many experiments. However, these field fluctuations occur on a time scale that is long compared to the duration between application of the first common $\pi/2$ pulse and the time of ion separation for detection, so we may employ the technique of spin echoes [24] to correct the dephasing. These $R_B(\pi, 0) \otimes R_A(\pi, 0)$ spin-echo pulses were inserted between the G_ϕ operations and the application of Bob's qubit encoding. They do not perfectly correct for field drifts due to the finite time for Bob to apply his operator, but they help suppress these dephasing effects. Aside from adding global phase factors, the spin-echo pulses do not change the protocol. Figure 1 schematically outlines the experiment, omitting the spin-echo pulses.

For each choice of Bob's operator, we measure the fidelity of the actual output state relative to the ideally expected output state

$$F = \langle \psi_{\text{ideal}} | \rho_{\text{out}} | \psi_{\text{ideal}} \rangle, \quad (5)$$

where ρ_{out} is the density matrix of the output state. These

TABLE I. Correlations between Bob's applied operator (top row) and Alice's state measurements of both qubits (left column). The entries correspond to the probabilities measured by Alice for each basis state. Ideally, the entries in bold should equal 1 and all other entries should equal zero.

	\tilde{I}	σ_y	σ_z	σ_x
$ \downarrow\rangle_B \downarrow\rangle_A$	0.84(2)	0.07(1)	0.08(1)	0.02(1)
$ \uparrow\rangle_B \downarrow\rangle_A$	0.07(1)	0.01(1)	0.84(1)	0.04(1)
$ \downarrow\rangle_B \uparrow\rangle_A$	0.06(1)	0.84(1)	0.04(1)	0.08(1)
$ \uparrow\rangle_B \uparrow\rangle_A$	0.03(1)	0.08(1)	0.04(1)	0.87(1)

data are included (in bold lettering) in Table I, where we also display the probabilities for detecting all other (undesired) states. Using the data from Table I, we calculate the channel capacity C with the use of Eq. (12.67) from Ref. [2], and find $C = 1.16(1)$. In the ideal situation, where no errors occur, we would find $C = 2.00$, corresponding to a channel capacity of two bits, as expected. In [3], two of Bob's operations could not be distinguished, so that only three states of classical information could be transferred (a "trit" vs two bits). Under ideal conditions, this would give a channel capacity of 1.58 bits. Our value for the channel capacity is only slightly above the value of 1.13 found in Ref. [3] for the case of trits, apparently due to the higher fidelity for each of the three detected operations [32]. However, in that experiment, only those transmissions where the appropriate coincidences were detected were used in the data analysis, whereas here, Table I entries are based on all experiments, without postselection.

In summary, we have implemented the quantum dense-coding protocol on atomic qubits using two trapped $^9\text{Be}^+$ ions. For the two bits of classical information encoded using quantum operations on a single qubit, we find an average transmission fidelity $\langle F \rangle = 0.85(1)$. We also determine a channel capacity $C = 1.16(1)$, which exceeds that which could be obtained in a perfect experiment (without entanglement) where a quantum bit is used to transmit classical information ($C = 1$). The techniques demonstrated here may eventually be useful for communication, but perhaps more significantly in the near term, they will facilitate the implementation of scalable quantum computation using trapped ions [17,33]. In the future, use of smaller trap electrodes to speed up ion separation and gate operations, coupled with better detection, should significantly increase the speed of such protocols.

This work was supported by ARDA/NSA under Contract No. MOD 7171.04 and by NIST. We thank J. Bollinger and P. Schmidt for helpful comments on the manuscript. T. S. acknowledges a Deutsche Forschungsgemeinschaft research grant. This paper is a contribution of the National Institute of Standards and Technology, not subject to U. S. copyright.

- *Present Address: Physics Department, Otago University, New Zealand.
- [1] C. H. Bennett and S. J. Wiesner, *Phys. Rev. Lett.* **69**, 2881 (1992).
- [2] M. A. Nielsen and I. L. Chuang, *Quantum Computation and Quantum Information* (Cambridge University Press, Cambridge, 2000), 1st ed.
- [3] K. Mattle, H. Weinfurter, P. G. Kwiat, and A. Zeilinger, *Phys. Rev. Lett.* **76**, 4656 (1996).
- [4] X. Fang *et al.*, *Phys. Rev. A* **61**, 022307 (2000).
- [5] M. Ban, *J. Opt. B Quantum Semiclassical Opt.* **1**, L9 (1999).
- [6] S. L. Braunstein and H. J. Kimble, *Phys. Rev. A* **61**, 042302 (1999).
- [7] T. C. Ralph and E. H. Huntington, *Phys. Rev. A* **66**, 042321 (2002).
- [8] X. Li *et al.*, *Phys. Rev. Lett.* **88**, 047904 (2002).
- [9] J. Mizuno, K. Wakui, A. Furusawa, and M. Sasaki, [quant-ph/0402040](http://arxiv.org/abs/quant-ph/0402040).
- [10] S. Bose, V. Vedral, and P. L. Knight, *Phys. Rev. A* **57**, 822 (1998).
- [11] J. C. Hao, C. F. Li, and G. C. Guo, *Phys. Rev. A* **63**, 054301 (2001).
- [12] H. J. Lee, D. Ahn, and S. W. Hwang, *Phys. Rev. A* **66**, 024304 (2002).
- [13] A. Wójcik and A. Grudka, *Phys. Rev. A* **68**, 016301 (2003).
- [14] O. Akhavan and A. T. Rezakhani, *Phys. Rev. A* **68**, 016302 (2003).
- [15] K. Shimizu, N. Imoto, and T. Mukai, *Phys. Rev. A* **59**, 1092 (1999).
- [16] See, for example, <http://qist.lanl.gov/>
- [17] D. J. Wineland *et al.*, *J. Res. Natl. Inst. Stand. Technol.* **103**, 259 (1998).
- [18] D. Kielpinski *et al.*, *Science* **291**, 1013 (2001).
- [19] A. Acín, E. Jané, and G. Vidal, *Phys. Rev. A* **64**, 050302 (2001).
- [20] A. M. Childs, J. Preskill, and J. Renes, *J. Mod. Opt.* **47**, 155 (2000).
- [21] J. I. Cirac, P. Zoller, H. J. Kimble, and H. Mabuchi, *Phys. Rev. Lett.* **78**, 3221 (1997).
- [22] In this context, we note that an eavesdropper intercepting the qubit sent from Bob to Alice could not gain any knowledge about the encoded message without access to the second qubit in the entangled pair. This would hold even for imperfect entanglement, as long as the imperfection is unbiased as, for example, a depolarizing error [M. A. Nielsen (private communication)].
- [23] R. P. Feynman, F. L. Vernon, and R. W. Hellwarth, *J. Appl. Phys.* **28**, 49 (1957).
- [24] L. Allen and J. H. Eberly, *Optical Resonance and Two-Level Atoms* (Dover, Mineola, NY, 1987).
- [25] M. A. Rowe *et al.*, *Quantum Inf. Comput.* **2**, 257 (2002).
- [26] B. E. King *et al.*, *Phys. Rev. Lett.* **81**, 1525 (1998).
- [27] The laser beam waists (approximately equal to the beam diameters) at the ions were approximately $30\ \mu\text{m}$, and the beam positions were adjusted to give equal intensity on both ions.
- [28] D. J. Wineland *et al.*, *Philos. Trans. R. Soc. London, Ser. A* **361**, 1349 (2003).
- [29] D. Leibfried *et al.*, *Nature (London)* **422**, 412 (2003).
- [30] M. A. Rowe *et al.*, *Nature (London)* **409**, 791 (2001).
- [31] In our previous experiments [25], the separation was achieved with only a 95% success probability and the motion was excited substantially, leading to poor detection efficiency. Aided by a smaller separation electrode in the current apparatus ($100\ \mu\text{m}$ wide vs $800\ \mu\text{m}$ wide in Ref. [25]), separation was accomplished with no detected failures and the small heating (about ten quanta) led to more efficient state detection.
- [32] From Ref. [3], we estimate the fidelity for the three cases using $F_i = (S/N)_i / [(S/N)_i + 1]$ and find $F_{|\Psi^+\rangle} \simeq 0.94$, $F_{|\Psi^-\rangle} \simeq 0.93$, and $F_{|\Phi^-\rangle} \simeq 0.90$.
- [33] D. Kielpinski, C. Monroe, and D. J. Wineland, *Nature (London)* **417**, 709 (2002).